Linear and Geometric Algebra Approaches for Sphere and Spherical Shell Intersections in $\mathbb{R}^n$

Carlile Lavor[a], Rafael Alves[b], Leandro A. F. Fernandes[c,*]

[a]*University of Campinas (IMECC-UNICAMP), ZIP 13081-970, Campinas-SP, Brazil*
[b]*Federal University of ABC (CMCC-UFABC), ZIP 09606-045, São Bernardo-SP, Brazil*
[c]*Fluminense Federal University (IC-UFF), ZIP 24210-346, Niterói-RJ, Brazil*

Abstract

Many practical problems involve sphere intersections. Examples include but are not limited to estimations using the Global Positioning System (GPS), data science applications and 3D protein structure determination. Motivated by practical situations, where radii of spheres are not known precisely, we consider what happens when a spherical shell must be included in the intersection. We present and compare two approaches for this problem: one uses linear algebra and the other is based on conformal geometric algebra (CGA). The theoretical development is illustrated with some numerical examples, where it is possible to note the main advantage of CGA compared to the linear algebra approach: even in dimensions higher than three, CGA naturally preserves the geometric intuition of the problem.

Keywords: sphere intersection, spherical shell intersection, conformal geometric algebra
2000 MSC: 68Q25, 68R10, 68U05

1. Introduction

Sphere intersections may appear as subproblems in many applications such as molecular and nanostructure geometry (Billinge et al., 2016, 2018), crystallography (Mackay, 1974), dimensionality reduction (Alencar et al., 2019), robotics (Nielsen and Roth, 1999), global positioning systems (Strang and Borre, 2012), and data science (Lavor, 2020; Liberti, 2020). In distance geometry (Liberti et al., 2014; Mucherino et al., 2013), sphere intersection is a fundamental step in solution methods (Cassioli et al., 2015a; Lavor et al., 2012a; Liberti et al., 2008) for problems related to calculating 3D protein structures using Nuclear Magnetic Resonance (NMR) data (Donald, 2011; Cassioli et al., 2015b; Lavor et al., 2012b, 2019).

---

[*]Corresponding author
Email addresses: `clavor@unicamp.br` (Carlile Lavor), `alves.rafael@ufabc.edu.br` (Rafael Alves), `laffernandes@ic.uff.br` (Leandro A. F. Fernandes)

When the radii of the spheres are not known precisely (which occurs in many practical situations), we can model these uncertainties using spherical shells, replacing precise radii with interval values (Gonçalves et al., 2017; Lavor et al., 2013; Malliavin et al., 2019; Lavor et al., 2021b; Worley et al., 2018; Lavor et al., 2020).

This paper generalizes a recent result involving the intersection of m spheres in $\mathbb{R}^n$ (Maioli et al., 2017), also considering a spherical shell in the intersection (Carielo and Fernandes, 2018). We present and compare two different approaches. The first one uses classical linear algebra (section 2.1), and the second is based on conformal geometric algebra (CGA) (section 2.2). Carielo (2019) initially described the second approach presented in this manuscript. This manuscript extends and corrects the original formulation and presents numerical examples to illustrate the theoretical development (section 3).

2. Methods

The following subsections describe the linear algebra approach (section 2.1) and the geometric algebra approach (section 2.2) for the intersection problem considered in this paper.

2.1. A linear algebra approach

An *i-sphere* in $\mathbb{R}^n$ is the intersection of a sphere with an affine subspace of dimension i. In (Maioli et al., 2017), the following theorem was presented.

Theorem 1. *Let $a_1, \cdots, a_m$ be the centers of m spheres in $\mathbb{R}^n$ whose respective radii are $d_1, \cdots, d_m \in \mathbb{R}$, for $m \geq 2$ and $n \geq 2$. If the affine hull of the sphere centers has dimension k, $1 \leq k \leq \min\{m-1, n\}$, then there are three possibilities for the sphere intersection: (1) the empty set; (2) a single point; and (3) an $(n-k)$-sphere.*

Theorem 2 extends theorem 1 by also considering a spherical shell in the intersection.

Theorem 2. *Let $a_1, \cdots, a_m$ be the centers of m spheres in $\mathbb{R}^n$ whose respective radii are $d_1, \cdots, d_m \in \mathbb{R}$, for $m \geq 2$ and $n \geq 2$, and $a_{m+1} \in \mathbb{R}^n$ the center of a spherical shell with radii $\underline{d}_{m+1}, \overline{d}_{m+1} \in \mathbb{R}$, where $0 < \underline{d}_{m+1} < \overline{d}_{m+1} \in \mathbb{R}$. If the affine hull of the set $\{a_1, \cdots, a_m\}$ has dimension k, $1 \leq k \leq \min\{m-1, n\}$, then there are four possibilities for the intersection between the spheres and the spherical shell: (1) the empty set; (2) a single point; (3) an $(n-k)$-sphere; and (4) a union of $(n-k-1)$-spheres.*

Proof 1. *The solution of the following system gives the intersection between the spheres and the spherical shell:*

$$||x - a_i||^2 = d_i^2, \quad for \; i = 1, \cdots, m, \tag{1a}$$

$$\underline{d}_{m+1}^2 \leq ||x - a_{m+1}||^2 \leq \overline{d}_{m+1}^2, \tag{1b}$$

where $||z||$ denotes the Euclidean norm throughout the paper. If $x \in \mathbb{R}^n$ satisfies eq. (1),

$$\overline{x} = x - a_m \tag{2}$$

is a solution for

$$||\overline{x} - (a_i - a_m)||^2 = d_i^2, \quad for\ i = 1, \cdots, m, \tag{3a}$$

$$\underline{d}_{m+1}^2 \leq ||\overline{x} - (a_{m+1} - a_m)||^2 \leq \overline{d}_{m+1}^2, \tag{3b}$$

which is equivalent to

$$||\overline{x}||^2 - 2\overline{x}^T(a_i - a_m) + ||a_i - a_m||^2 = d_i^2, \quad for\ i = 1, \cdots, m, \tag{4a}$$

$$\underline{d}_{m+1}^2 \leq ||\overline{x}||^2 - 2\overline{x}^T(a_{m+1} - a_m) + ||a_{m+1} - a_m||^2 \leq \overline{d}_{m+1}^2. \tag{4b}$$

For $i = m$, in eq. (3a), we have $||\overline{x}||^2 = d_m^2$ which means that eq. (4) can be written as

$$(a_i - a_m)^T\overline{x} = -\frac{1}{2}\left(d_i^2 - d_m^2 - ||a_i - a_m||^2\right), \quad for\ i = 1, \cdots, m-1,$$

$$-\frac{1}{2}\left(\overline{d}_{m+1}^2 - d_m^2 - ||a_{m+1} - a_m||^2\right) \leq (a_{m+1} - a_m)^T\overline{x} \leq -\frac{1}{2}\left(\underline{d}_{m+1}^2 - d_m^2 - ||a_{m+1} - a_m||^2\right),$$

and simplified to

$$\overline{a}_i^T\overline{x} = c_i, \quad for\ i = 1, \cdots, m-1, \tag{6a}$$

$$\underline{c}_m \leq \overline{a}_m^T\overline{x} \leq \overline{c}_m, \tag{6b}$$

where

$$\overline{a}_i = a_i - a_m, \quad for\ i = 1, \cdots, m-1, \tag{7a}$$

$$c_i = -\frac{1}{2}\left(d_i^2 - d_m^2 - ||a_i - a_m||^2\right), \quad for\ i = 1, \cdots, m-1, \tag{7b}$$

$$\overline{a}_m = a_{m+1} - a_m, \tag{7c}$$

$$\underline{c}_m = -\frac{1}{2}\left(\overline{d}_{m+1}^2 - d_m^2 - ||a_{m+1} - a_m||^2\right), \tag{7d}$$

$$\overline{c}_m = -\frac{1}{2}\left(\underline{d}_{m+1}^2 - d_m^2 - ||a_{m+1} - a_m||^2\right). \tag{7e}$$

Now, we have to deal with two cases for the dimension of the affine hull of the set $\{a_1, \cdots, a_m, a_{m+1}\}$. Let us consider first that this dimension is k, which implies that the matrix whose columns are defined by vectors in eq. (7a) and eq. (7c), given by

$$A = \begin{bmatrix} \overline{a}_1 & \cdots & \overline{a}_m \end{bmatrix}, \tag{8}$$

has rank also equal to k.

Computing the QR decomposition (Golub and van Loan, 1996) of A, we obtain

$$A = Q\begin{bmatrix} R & r \\ 0 & 0 \end{bmatrix},$$

where $Q \in \mathbb{R}^{n \times n}$ is orthogonal, $R \in \mathbb{R}^{k \times (m-1)}$ has full rank, and $r \in \mathbb{R}^k$, implying that

$$A^T \overline{x} = \begin{bmatrix} R^T & 0 \\ r^T & 0 \end{bmatrix} Q^T \overline{x}. \tag{9}$$

Writing $Q^T \overline{x}$ as

$$Q^T \overline{x} = \begin{bmatrix} y \\ z \end{bmatrix},$$

with $y \in \mathbb{R}^k$ and $z \in \mathbb{R}^{n-k}$, from eq. (2), we get

$$x = Q \begin{bmatrix} y \\ z \end{bmatrix} + a_m.$$

From eq. (6) and eq. (9), the vector y must satisfy

$$R^T y = c, \tag{10a}$$

$$\underline{c}_m \leq r^T y \leq \overline{c}_m, \tag{10b}$$

where $c = (c_1, \cdots, c_{m-1})^T$. If there is no solution for eq. (10a), the solution set for eq. (1) is empty. However, since R^T has full rank, if there is a solution y satisfying eq. (10), this solution is unique.

From eq. (1), for $i = m$, we have

$$||x - a_m||^2 = \left\| Q \begin{bmatrix} y \\ z \end{bmatrix} \right\|^2 = \left\| \begin{bmatrix} y \\ z \end{bmatrix} \right\|^2 = d_m^2,$$

which means that

$$z_1^2 + \cdots + z_{n-k}^2 = \rho^2,$$

where $\rho^2 = d_m^2 - ||y||^2$. Thus, we obtain three possibilities for the solution of eq. (1): (1) the empty set, if $\rho^2 < 0$; (2) a single point, if $\rho^2 = 0$; and (3) an $(n-k)$-sphere, if $\rho^2 > 0$.

Now, if we assume that the dimension of the affine hull of the set $\{a_1, \cdots, a_m, a_{m+1}\}$ is $k+1$, the same matrix A defined in eq. (8), i.e.,

$$A = \begin{bmatrix} \overline{a}_1 & \cdots & \overline{a}_m \end{bmatrix},$$

has rank equal to $k+1$.

Let E be the permutation matrix that puts the column $\overline{a}_m$ of A in the position $k+1$. Computing the QR decomposition of AE, we obtain

$$AE = Q\mathcal{R} = Q \begin{bmatrix} R & r \\ 0 & r_{k+1} \\ 0 & 0 \end{bmatrix}, \tag{11}$$

where $Q \in \mathbb{R}^{n \times n}$ is orthogonal, $R \in \mathbb{R}^{k \times (m-1)}$ has full rank, $r \in \mathbb{R}^k$, and $r_{k+1} \in \mathbb{R}$.

Since $E^T = E^{-1}$, we get

$$(AE)^T = (Q\mathcal{R})^T \Rightarrow A^T = E\mathcal{R}^T Q^T,$$

which implies that, from eq. (11),

$$A^T \overline{x} = E\mathcal{R}^T Q^T \overline{x} = \begin{bmatrix} R^T & 0 & 0 \\ r^T & r_{k+1} & 0 \end{bmatrix} Q^T \overline{x}. \tag{12}$$

Writing $Q^T \overline{x}$ as

$$Q^T \overline{x} = \begin{bmatrix} y \\ y_{k+1} \\ z \end{bmatrix}, \tag{13}$$

where $y \in \mathbb{R}^k$, $y_{k+1} \in \mathbb{R}$, and $z \in \mathbb{R}^{n-k-1}$, from eq. (6) and eq. (12), y and y_{k+1} must satisfy

$$R^T y = c,$$

$$\underline{c}_m \leq \begin{bmatrix} r^T & r_{k+1} \end{bmatrix} \begin{bmatrix} y \\ y_{k+1} \end{bmatrix} \leq \overline{c}_m,$$

where $c = (c_1, \cdots, c_{m-1})^T$, which is equivalent to

$$R^T y = c, \tag{15a}$$

$$\underline{c}_m - r^T y \leq r_{k+1} y_{k+1} \leq \overline{c}_m - r^T y. \tag{15b}$$

If there is no solution for eq. (15a), the solution set for eq. (1) is empty. However, since R^T has full rank, if there is a solution y satisfying eq. (15a), this solution is unique.

From eq. (15b), we get

$$\underline{\alpha} \leq y_{k+1} \leq \overline{\alpha}, \tag{16}$$

where

$$\underline{\alpha} = \frac{\underline{c}_m - r^T y}{r_{k+1}} \quad and \quad \overline{\alpha} = \frac{\overline{c}_m - r^T y}{r_{k+1}}, \quad if \ r_{k+1} > 0,$$

$$\underline{\alpha} = \frac{\overline{c}_m - r^T y}{r_{k+1}} \quad and \quad \overline{\alpha} = \frac{\underline{c}_m - r^T y}{r_{k+1}}, \quad if \ r_{k+1} < 0.$$

From eq. (2) and eq. (13), we have

$$x = Q \begin{bmatrix} y \\ y_{k+1} \\ z \end{bmatrix} + a_m, \tag{18}$$

and replacing eq. (18) in eq. (1a), for $i = m$, we obtain

$$\left\| Q \begin{bmatrix} y \\ y_{k+1} \\ z \end{bmatrix} \right\|^2 = \left\| \begin{bmatrix} y \\ y_{k+1} \\ z \end{bmatrix} \right\|^2 = d_m^2,$$

which is equivalent to

$$||z||^2 = d_m^2 - ||y||^2 - y_{k+1}^2. \tag{19}$$

5

Equation (19) has a real solution $||z||$ if and only if

$$d_m^2 - ||y||^2 - y_{k+1}^2 \geq 0. \tag{20}$$

There is no real solution for eq. (19) when $d_m^2 - ||y||^2 < 0$. If $d_m^2 - ||y||^2 \geq 0$. Then the inequality in eq. (20) can be written as

$$-\beta \leq y_{k+1} \leq \beta, \tag{21}$$

where $\beta = \sqrt{d_m^2 - ||y||^2}$. From eq. (16) and eq. (21),

$$y_{k+1} \in [\underline{\alpha}, \overline{\alpha}] \cap [-\beta, \beta],$$

which means that

$$\max\{\underline{\alpha}, -\beta\} \leq y_{k+1} \leq \min\{\overline{\alpha}, \beta\}. \tag{22}$$

Thus, from the unique solution y of eq. (15a), for each y_{k+1} satisfying a non-degenerate interval (eq. (22)) and z satisfying eq. (19), eq. (18) gives an $(n-k-1)$-sphere. Considering all values y_{k+1} satisfying eq. (22), the result is a union of $(n-k-1)$-spheres.

2.2. A geometric algebra approach

The *conformal model* can also represent the Euclidean space $\mathbb{R}^n$, augmenting the space with two extra dimensions, e_0 and e_∞, representing, respectively, the point at the origin and the point at infinity, and a new metric defined for $\mathbb{R}^{n+2}$ as:

$$e_i \cdot e_j = \delta_{ij},$$
$$e_0 \cdot e_i = e_\infty \cdot e_i = 0,$$
$$e_0 \cdot e_0 = e_\infty \cdot e_\infty = 0,$$
$$e_0 \cdot e_\infty = -1,$$

for $i, j = 1, \cdots, n$. Here, δ_{ij} is the well-known Kronecker delta. Note that the usual Euclidean metric still holds for $e_1, \cdots, e_n$. Please refer to (Kanatani, 2015) for an in-depth discussion on the metric of the conformal model.

The metric defined by this inner product does not satisfy the positivity of the usual inner product but satisfies the other properties for $\alpha \in \mathbb{R}$ and $u, v, w \in \mathbb{R}^{n+2}$:

$$u \cdot v = v \cdot u,$$
$$u \cdot (v + w) = (u \cdot v) + (u \cdot w),$$
$$\alpha(u \cdot v) = (\alpha u) \cdot v = u \cdot (\alpha v).$$

The conformal model has its origin in the work of F. Wachter, a student of Gauss, who showed that a specific subset of $\mathbb{R}^{n+2}$, called the *horosphere*, is metrically equivalent to $\mathbb{R}^n$ (Li et al., 2001). Dress and Havel (2014) provide a comprehensive discussion on the subject. The horosphere is defined by

$$X \cdot X = 0$$

6

and
$$(X - e_0) \cdot e_\infty = 0,$$

which implies that
$$X = x + e_0 + \frac{1}{2}||x||^2 e_\infty,$$

where $X \in \mathbb{R}^{n+2}$ is the conformal representation of $x \in \mathbb{R}^n$ (Li et al., 2001).

Using this representation for $x, y \in \mathbb{R}^n$, we obtain

$$\begin{aligned} X \cdot Y &= \left(x + e_0 + \frac{1}{2}||x||^2 e_\infty \right) \cdot \left(y + e_0 + \frac{1}{2}||y||^2 e_\infty \right) \\ &= x \cdot y - \left(\frac{1}{2}||x||^2 + \frac{1}{2}||y||^2 \right) \\ &= -\frac{1}{2}||x - y||^2, \end{aligned}$$

implying that the inner product $X \cdot Y$ is the squared Euclidean distance between x and y, up to a constant factor.

From this fact, a sphere in $\mathbb{R}^n$ can be represented by a vector $\sigma \in \mathbb{R}^{n+2}$, given by
$$\sigma = C - \frac{r^2}{2} e_\infty,$$

where C is the conformal representation of the sphere center $c \in \mathbb{R}^n$ and $r \in \mathbb{R}$ is its radius. To see this, we use the property

$$X \cdot e_\infty = \left(x + e_0 + \frac{1}{2}||x||^2 e_\infty \right) \cdot e_\infty = -1$$

to get

$$X \cdot \sigma = X \cdot \left(C - \frac{r^2}{2} e_\infty \right) = X \cdot C - \frac{r^2}{2}(X \cdot e_\infty) = -\frac{1}{2}||x - c||^2 + \frac{r^2}{2},$$

which implies that
$$X \cdot \sigma = 0 \Leftrightarrow ||x - c||^2 = r^2.$$

The conformal model can also represent sphere intersections if another associative and distributive product, called *outer product* (Kanatani, 2015), is introduced by

$$\begin{aligned} e_i \wedge e_j &= -e_j \wedge e_i, \\ e_i \wedge e_0 &= -e_0 \wedge e_i, \\ e_i \wedge e_\infty &= -e_\infty \wedge e_i, \\ e_0 \wedge e_\infty &= -e_\infty \wedge e_0, \\ e_i \wedge e_i = e_0 \wedge e_0 &= e_\infty \wedge e_\infty = 0, \end{aligned}$$

for $i, j = 1, \cdots, n$.

In fact, the inner and outer products can be defined in terms of a more general associative and distributive product, called *geometric product* (Kanatani, 2015), given by:

$$e_i e_j + e_j e_i = 2\delta_{ij},$$
$$e_0 e_i = -e_i e_0,$$
$$e_\infty e_i = -e_i e_\infty,$$
$$e_0^2 = e_\infty^2 = 0,$$
$$e_0 e_\infty + e_\infty e_0 = -2,$$

where $a \cdot b = \frac{1}{2}(ab + ba)$ and $a \wedge b = \frac{1}{2}(ab - ba)$, for $a, b \in \mathbb{R}^{n+2}$ and $i, j = 1, \cdots, n$.

Before presenting the second approach, we need an important result from CGA, given in (Dorst et al., 2007; Perwass, 2009) and presented by theorem 3.

Theorem 3. *Let m spheres in $\mathbb{R}^n$ with different centers $a_1, \cdots, a_m \in \mathbb{R}^n$ ($m \geq 2$ and $n \geq 2$), where the affine hull of the set $\{a_1, \cdots, a_m\}$ has dimension k, $1 \leq k \leq \min\{m-1, n\}$. If the conformal representations of the associated m spheres are $\sigma_1, \cdots, \sigma_m \in \mathbb{R}^{n+2}$, the intersection σ of these spheres is given by $\sigma = \bigwedge_{i=1}^m \sigma_i$, with $t = \sigma \cdot \tilde{\sigma}$ and $\tilde{\sigma} = (-1)^{m(m-1)/2}\sigma$, such that:*

- *If $t < 0$, then σ is an imaginary $(n-k)$-sphere representing the empty set;*

- *If $t = 0$, then σ is a single point;*

- *If $t > 0$, then σ is an $(n-k)$-sphere.*

When $t > 0$, t is proportional to the squared radius of the resulting $(n-k)$-sphere in $\mathbb{R}^n$, with center C_σ and radius r_σ given respectively by

$$C_\sigma = -\frac{1}{2}\frac{\sigma e_\infty \sigma}{(e_\infty \cdot \sigma)^2} \quad and \quad r_\sigma^2 = \frac{(-1)^{(m+1)}\sigma^2}{(e_\infty \cdot \sigma)^2}.$$

To calculate the intersection between the $(n-k)$-sphere (supposing $t > 0$)

$$\sigma = \bigwedge_{i=1}^m \sigma_i$$

and the spherical shell

$$s = A_{m+1} - \frac{d^2}{2}e_\infty, \quad d \in [\underline{d}_{m+1}, \overline{d}_{m+1}],$$

let us define two additional spheres given by

$$\underline{s} = A_{m+1} - \frac{\underline{d}_{m+1}^2}{2}e_\infty \quad and \quad \overline{s} = A_{m+1} - \frac{\overline{d}_{m+1}^2}{2}e_\infty.$$

For the intersections $\sigma_L = \sigma \wedge \underline{s}$ and $\sigma_U = \sigma \wedge \overline{s}$, we just calculate

$$\underline{t} = \sigma_L \cdot \tilde{\sigma}_L \quad and \quad \overline{t} = \sigma_U \cdot \tilde{\sigma}_U. \tag{24}$$
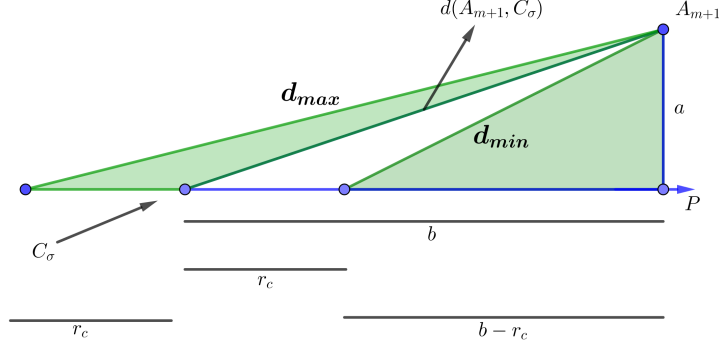
Figure 1: The horizontal line lies in the hyperplane $e_\infty \cdot \sigma$ containing σ and passes through its center; a is the distance between A_{m+1} and its orthogonal projection P; b is the distance from the projection to the C_σ; r_c is the radius of σ; d_{min} and d_{max} are the minimum and maximum distances between A_{m+1} and σ.

We have to check if $\underline{d}_{m+1}, \overline{d}_{m+1}$ should be updated for negative values of $\underline{t}, \overline{t}$, calculating the maximum and minimum distances between A_{m+1} and σ.

For this calculation, we need to project A_{m+1} on the hyperplane $\sigma_P = e_\infty \cdot \sigma$ associated with σ (Dorst et al., 2007) (see fig. 1), given by

$$P = (A_{m+1} \cdot \sigma_P^{-1})\sigma_P,$$

and calculate the distance $d(A_{m+1}, P)$ between A_{m+1} and P (see fig. 1), given by

$$a = d(A_{m+1}, P) = A_{m+1} \cdot P,$$

since P is a plane[1] (Hildenbrand, 2012). From a and $d(A_{m+1}, C_\sigma)$, given by

$$d(A_{m+1}, C_\sigma) = \sqrt{-2(A_{m+1} \cdot C_\sigma)},$$

we easily obtain the distance b between C_σ and the projected point (see fig. 1), given by

$$b = \sqrt{d(A_{m+1}, C_\sigma)^2 - a^2}.$$

Now, considering the radius r_σ of σ, we have (see fig. 1)

$$d_{\min} = \sqrt{a^2 + (b - r_\sigma)^2} \quad \text{and} \quad d_{\max} = \sqrt{a^2 + (b + r_\sigma)^2}.$$

Hence, the interval $[\underline{d}_{m+1}, \overline{d}_{m+1}]$ must be updated according to the following conditions:

- If $\underline{t} < 0$ and $\underline{d}_{m+1} < d_{\min}$, then $\underline{d}_{m+1} := d_{\min}$,

---

[1]A plane is given by $\Pi = \mathbf{n} + de_\infty$, where $\mathbf{n} \in \mathbb{R}^n$ is its unitary normal vector and d is its distance to the origin. To normalize an arbitrary plane, we divide it by $||\mathbf{n}||$. We are considering that P is normalized.

- If $\bar{t} < 0$ and $\bar{d}_{m+1} > d_{\max}$, then $\bar{d}_{m+1} := d_{\max}$.

The final result is then an union of $(n - k - 1)$-spheres, given by

$$\{\tau_d \in \mathbb{R}^{n+2} : \tau_d = \sigma \wedge s, d \in [\underline{d}_{m+1}, \bar{d}_{m+1}]\},$$

where $s = A_{m+1} - \frac{d^2}{2} e_\infty$.

From the proof of theorem 2, we can define an algorithm to compute the intersection between the spheres and the spherical shell using $\frac{2}{3}m^3 + \frac{5}{2}m^2$ additions/subtractions and multiplications and m squared roots when Householder transformations calculate the QR factors (Coope, 2000). According to Camargo et al. (2019), the number of arithmetic operations required, assuming naive implementations of the CGA approach, on the other hand, would be impractical, in the order of $m!$ operations (see (Camargo et al., 2019, eq. (24))). However, Camargo et al. also emphasize that this complexity issue is not intrinsic to the CGA. It is related to how most computational libraries implement CGA operations based on the multivector representation of their primitives. Fortunately, recent computational libraries, such as TbGAL (Sousa and Fernandes, 2020), apply more viable techniques for implementing CGA for high dimensional spaces, reducing the computational cost of intersecting m spheres to the same complexity as using the QR decomposition of matrices while keeping the high-level geometric intuition of CGA solutions (Buchanan, 2011).

3. Results

To illustrate the differences between the two approaches, let us consider two examples. In order to have a visualization of the problem, we consider first an example in the 3D space. The second example is given in $\mathbb{R}^5$. Although it is no longer possible to depict this case, the calculations presented for the CGA approach follow the same geometric intuition used in $\mathbb{R}^3$. In fact, the methodology is the same for the general case in $\mathbb{R}^n$.

3.1. Example 1

In the first example, $n = 3$, $m = 2$, and $k = 1$. The two spheres in $\mathbb{R}^3$ have centers and radii respectively given by

$$a_1 = (-4, 0, 0)^T, \qquad\qquad d_1 = 3.1102,$$
$$a_2 = (-3, -1.1133, 1.3268)^T, \qquad\qquad d_2 = 1.3,$$

and the spherical shell has center and interval radius

$$a_3 = (0, 0, 0)^T, \qquad\qquad d_3 \in [\underline{d}_3, \bar{d}_3] = [1.5, 3.7].$$

The matrix AE is given by

$$AE = \begin{bmatrix} -1 & 3 \\ 1.1133 & -1.1133 \\ -1.3268 & -1.3268 \end{bmatrix}$$

and its QR decomposition (eq. (11)) is

$$
Q \begin{bmatrix} R & r \\ 0 & r_{k+1} \\ 0 & 0 \end{bmatrix} = \begin{bmatrix} -0.5001 & -0.866019 & 0 \\ 0.556661 & -0.321397 & 0.766049 \\ -0.663414 & 0.383033 & 0.642782 \end{bmatrix} \begin{bmatrix} 1.99996 & -0.0000824367 \\ 0 & -3.46408 \\ 0 & 0 \end{bmatrix}.
$$

The system in eq. (15a) is given by

$$
1.99996y = -1.99175 \Rightarrow y = -0.995898.
$$

Since $r_2 = -3.46408 < 0$ and $d_2^2 - ||y||^2 = 0.698188 \geq 0$, we obtain

$$
y_2 \in [\underline{\alpha}, \overline{\alpha}] = [-1.6512, 0.0000475] \quad \text{and} \quad \beta = 0.8356,
$$

which implies that

$$
\max\{-1.6512, -0.8356\} \leq y_2 \leq \min\{0.0000475, 0.8356\} \Leftrightarrow -0.8356 \leq y_2 \leq 0.0000475.
$$

From eq. (18), all the solutions for eq. (1) are given by

$$
x = \begin{bmatrix} -0.5001 & -0.866019 & 0 \\ 0.556661 & -0.321397 & 0.766049 \\ -0.663414 & 0.383033 & 0.642782 \end{bmatrix} \begin{bmatrix} -0.995898 \\ y_2 \\ \pm\sqrt{0.69819 - y_2^2} \end{bmatrix} + \begin{bmatrix} -3 \\ -1.1133 \\ 1.3268 \end{bmatrix},
$$

where $y_2 \in [-0.8356, 0.0000475]$.

For $y_2 = -0.8356$, we obtain, from eq. (19),

$$
||z||^2 = -||y||^2 - y_2^2 + d_2^2 \Leftrightarrow ||z||^2 = -0.995898 - 0.69819 + 1.69 = 0, \quad (25)
$$

and, from eq. (18),

$$
x = Q \begin{bmatrix} y \\ y_2 \\ z \end{bmatrix} + a_2 = \begin{bmatrix} -1.77842 \\ -1.39913 \\ 1.66744 \end{bmatrix},
$$

implying that

$$
\begin{aligned}
||x - a_1|| &= 3.1102, \\
||x - a_2|| &= 1.3, \\
||x - a_3|| &= 2.81081 \in [1.5, 3.7].
\end{aligned}
$$

For $y_2 = 0.0000475$, we get two points given by

$$
(-2.50208, -1.02760, 2.52460)^T
$$

and

$$
(-2.50208, -2.30779, 1.45042)^T.
$$

For the second approach, we first calculate the intersection

$$
\sigma = \sigma_1 \wedge \sigma_2 = \left(c_1 - \frac{d_1^2}{2} e_\infty \right) \wedge \left(c_2 - \frac{d_2^2}{2} e_\infty \right)
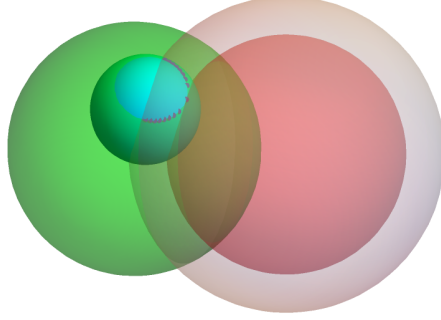$$

11

Figure 2: The solution of Example 1 is an arc delimited by the spherical shell on the circle resulting from the intersection of spheres σ_1 and σ_2. Here, the green and blue spheres correspond to σ_1 and σ_2. The red spheres represent the spherical shell.

and $t = \sigma \cdot \tilde{\sigma} = 2.7926$. Since $t > 0$, the intersection is a circle, with center c_σ and radius r given respectively by

$$c_\sigma = [-2.50204, -1.66768, 1.98749]^T,$$
$$r_\sigma = 0.8356.$$

From eq. (24), we obtain $\underline{t} < 0$ and $\bar{t} > 0$, leading to $d_{\min} = 2.81081$ and $d_{\max} = 4.41346$, which implies that $\underline{d}_3$ must be updated.

Thus, the solution is an arc given by

$$\{\tau_d \in \mathbb{R}^5 : \tau_d = \sigma \wedge s, \quad d \in [2.81081, 3.7]\},$$

where $s = A_3 - \frac{d^2}{2}e_\infty$.

Figure 2 illustrates the solution for some values in the interval $[2.81081, 3.7]$.

3.2. Example 2

Now, $n = 5$, $m = 4$, $k = 3$, and the problem is calculating the intersection of four spheres in $\mathbb{R}^5$, whose centers and radii are given by, respectively,

$$a_1 = (3.90254, 0.449824, 2.62402, 2.40872, 2.69034)^T, \qquad d_1 = 103.094,$$
$$a_2 = (2.10451, 0.219446, 1.64722, 0.647672, 1.02606)^T, \qquad d_2 = 105.419,$$
$$a_3 = (5.69087, 3.03019, 5.877, 2.76247, 6.22112)^T, \qquad d_3 = 98.7719,$$
$$a_4 = (2.71275, 2.75676, 3.76752, 1.33933, 4.50268)^T, \qquad d_4 = 101.787,$$

with a spherical shell whose center and interval radius are

$$a_5 = (37.3536, 56.5973, 33.8977, 61.2998, 38.2571)^T, \qquad d_5 \in [\underline{d}_5, \bar{d}_5] = [13.2591, 33.2127].$$

The matrix AE is given by

$$AE = \begin{bmatrix} 1.18979 & -0.60824 & 2.97812 & 34.6409 \\ -2.30694 & -2.53731 & 0.27343 & 53.8405 \\ -1.1435 & -2.1203 & 2.10948 & 30.1302 \\ 1.06939 & -0.691658 & 1.42314 & 59.9605 \\ -1.81234 & -3.47662 & 1.71844 & 33.7544 \end{bmatrix}$$

and its QR decomposition has

$$Q = \begin{bmatrix} -0.336883 & -0.585671 & -0.505052 & -0.068026 & -0.532723 \\ 0.653198 & -0.035156 & 0.049021 & -0.676614 & -0.334493 \\ 0.323776 & -0.289147 & -0.58995 & -0.050785 & 0.678928 \\ -0.302792 & -0.57207 & 0.5502 & -0.395397 & 0.349278 \\ 0.513155 & -0.494854 & 0.302918 & 0.615343 & -0.146227 \end{bmatrix}$$

and

$$\mathcal{R} = \begin{bmatrix} R & r \\ 0 & r_{k+1} \\ 0 & 0 \end{bmatrix} = \begin{bmatrix} -3.53176 & -3.71358 & 0.30924 & 32.4197 \\ 0 & 3.17462 & -4.02828 & -81.8983 \\ 0 & 0 & -1.43163 & 10.5836 \\ 0 & 0 & 0 & -43.2534 \\ 0 & 0 & 0 & 0 \end{bmatrix}.$$

The solution of the system in eq. (15a) is given by

$$y = (36.1443, -72.4896, -5.83463)^T,$$

where $c = (-127.653, -364.352, 311.539)^T$.

Since $r_4 = -43.2534 < 0$ and $d_4^2 - ||y||^2 = 3765.39 \geq 0$, we obtain

$$y_4 \in [\underline{\alpha}, \overline{\alpha}] = [-67.4211, -56.7022] \quad \text{and} \quad \beta = 61.3628,$$

which implies that

$$\max\{-67.4211, -61.3628\} \leq y_4 \leq \min\{-56.7022, 61.3628\} \Leftrightarrow -61.3628 \leq y_4 \leq -56.7022.$$

Therefore, according to eq. (25), all the solutions for eq. (1) are given by

$$x = \begin{bmatrix} -0.3369 & -0.5857 & -0.5050 & -0.0680 & -0.5327 \\ 0.6532 & -0.0352 & 0.0490 & -0.6766 & -0.3345 \\ 0.3238 & -0.2892 & -0.590 & -0.0508 & 0.6789 \\ -0.3028 & -0.5721 & 0.5502 & -0.3954 & 0.3493 \\ 0.5132 & -0.4948 & 0.3030 & 0.6153 & -0.1462 \end{bmatrix} \begin{bmatrix} 36.1443 \\ -72.4896 \\ -5.8346 \\ y_4 \\ \pm\sqrt{3765.39 - y_4^2} \end{bmatrix} + \begin{bmatrix} 2.7128 \\ 2.7568 \\ 3.7675 \\ 1.3393 \\ 4.5027 \end{bmatrix},$$

where $y_4 \in [-61.3628, -56.7022]$.

For $y_4 = -56.702$, for example, we obtain two possible solutions for x,

$$(52.2918, 74.8406, 26.8265, 42.8805, 25.6935)^T$$

and
$$(27.2992, 59.1478, 58.6782, 59.2669, 18.8334)^T,$$

implying that

$$\|x - a_1\| = 103.094,$$
$$\|x - a_2\| = 105.419,$$
$$\|x - a_3\| = 98.7719,$$
$$\|x - a_4\| = 101.787,$$
$$\|x - a_5\| = 33.2127 \in [13.2591, 33.2127].$$

And for $y_4 = -61.3628$, we have $\sqrt{3765.39 - y_4^2} = 0$, so we obtain just one possibility for x,

$$(40.1125, 70.1476, 42.9890, 52.9165, 19.3955)^T$$

with

$$\|x - a_5\| = 26.4559 \in [13.2591, 33.2127].$$

For the second approach, we first calculate the intersection

$$\sigma = \sigma_1 \wedge \sigma_2 \wedge \sigma_3 \wedge \sigma_4$$
$$= \left(A_1 - \frac{d_1^2}{2} e_\infty \right) \wedge \left(A_2 - \frac{d_2^2}{2} e_\infty \right) \wedge \left(A_3 - \frac{d_3^2}{2} e_\infty \right) \wedge \left(A_4 - \frac{d_4^2}{2} e_\infty \right)$$

and $t = 970144.57$. Since $t > 0$, the intersection is a 2-sphere with center c_σ and radius r_σ given respectively by

$$c_\sigma = [35.9383, 28.6286, 39.8725, 28.6540, 57.1548]^T,$$
$$r_\sigma = 61.3628.$$

From eq. (24), we obtain $\underline{t} = -3.761 < 0$ and $\bar{t} = 2.652 > 0$, leading to $d_{\min} = 26.4559$ and $d_{\max} = 106.379$, which implies that $\underline{d}_5$ must be updated.

Thus, the solution is given by

$$\{\tau_d \in \mathbb{R}^5 : \tau_d = \sigma \wedge s, d \in [26.4559, 33.2127]\},$$

where $s = A_5 - \frac{d^2}{2} e_\infty$.

For $d = 33.2127$, we obtain two solutions,

$$(52.2918, 74.8406, 26.8265, 42.8805, 25.6935)^T$$

and

$$(27.2992, 59.1478, 58.6782, 59.2669, 18.8334)^T.$$

For $d = 26.4559$, we obtain a single solution, given by

$$(40.1125, 70.1476, 42.9890, 52.9165, 19.3955)^T.$$

Notice that those are the same results obtained by the linear algebra approach.

4. Conclusion

Spheres and spherical shells are fundamental objects in the conformal model of the Euclidean space $\mathbb{R}^n$ that can be easily manipulated using the language of CGA. Some results related to molecular geometry are given in (Alves and Lavor, 2017; Alves et al., 2018; Camargo et al., 2019; Lavor and Alves, 2019; Lavor et al., 2021a).

The computational cost of the presented CGA approach is related to the outer product between spheres, which can be kept equivalent to the use of QR decomposition if efficient implementations of geometric algebra for high dimensionalities are employed (*e.g.,* (Sousa and Fernandes, 2020)).

Compared to the linear algebra approach, CGA seems to be a language more suitable to deal with the natural extension of this paper, where the intersection should include many spherical shells. As stated by Richard Feynman (Buchanan, 2011), the history of mathematics is largely the history of improvements in notation. We believe the compact notation of geometric algebra and its intrinsic geometric intuition, allied to the efficient implementation of CGA for high-dimensions, are invaluable tools to find solutions not yet foreseen for problems that require the intersection of spherical shells.

In addition to the theoretical development given to the problem of spheres and spherical shell intersections, this paper also presented computational experiments to compare the two proposed approaches. According to our observations, the main advantage of CGA compared to the linear algebra approach is that even in dimensions higher than three, CGA naturally preserves the geometric intuition of the problem's solution.

References

Alencar, J., Lavor, C., Liberti, L., 2019. Realizing Euclidean distance matrices by sphere intersection. Discrete Applied Mathematics 256, 5–10.

Alves, R., Lavor, C., 2017. Geometric algebra to model uncertainties in the discretizable molecular distance geometry problem. Advances in Applied Clifford Algebra 27, 439–452.

Alves, R., Lavor, C., Souza, C., Souza, M., 2018. Clifford algebra and discretizable distance geometry. Mathematical Methods in the Applied Sciences 41, 4063–4073.

Billinge, S., Duxbury, P., Gonçalves, D., Lavor, C., Mucherino, A., 2016. Assigned and unassigned distance geometry: applications to biological molecules and nanostructures. 4OR 14, 337–376.

Billinge, S., Duxbury, P., Gonçalves, D., Lavor, C., Mucherino, A., 2018. Recent results on assigned and unassigned distance geometry with applications to protein molecules and nanostructures. Annals of Operations Research 271, 161–203.

Buchanan, M., 2011. Geometric intuition. Nature Physics 7, 442.

Camargo, V., Castelani, E., Fernandes, L.A.F., Fidalgo, F., 2019. Geometric algebra to describe the exact discretizable molecular distance geometry problem for an arbitrary dimension. Advances in Applied Clifford Algebra 29, 75.

Carielo, M.S., 2019. Interseção de esferas e álgebra geométrica. Ph.D. thesis. IMECC - Universidade Estadual de Campinas. In Portuguese.

Carielo, M.S., Fernandes, L.A.F., 2018. Using conformal geometric algebra to determine the structure of proteins with uncertainties, in: Early Proceedings of the AGACSE 2018 Conference, pp. 197–198.

Cassioli, A., Bordeaux, B., Bouvier, G., Mucherino, A., R.Alves, Liberti, L., Nilges, M., Lavor, C., Malliavin, T., 2015a. An algorithm to enumerate all possible protein conformations verifying a set of distance constraints. BMC Bioinformatics 16, 16–23.

Cassioli, A., Gunluk, O., Lavor, C., Liberti, L., 2015b. Discretization vertex orders in distance geometry. Discrete Applied Mathematics 197, 27–41.

Coope, I., 2000. Reliable computation of the points of intersection of n spheres in $\mathbb{R}^n$, in: Proceedings Computational Techniques and Applications Conference, pp. 461–477.

Donald, B., 2011. Algorithms in structural molecular biology. MIT Press.

Dorst, L., Fontijne, D., Mann, S., 2007. Geometric algebra for computer science: an object-oriented approach to geometry. Morgan Kaufman.

Dress, A., Havel, T.F., 2014. Distance geometry and geometric algebra. Foundations of Physics 23, 1357–1374.

Golub, G., van Loan, C., 1996. Matrix computations. 3 ed., JHU Press.

Gonçalves, D., Mucherino, A., Lavor, C., Liberti, L., 2017. Recent advances on the interval distance geometry problem. Journal of Global Optimization 69, 525–545.

Hildenbrand, D., 2012. Foundations of geometric algebra computing. Springer.

Kanatani, K., 2015. Understanding geometric algebra: Hamilton, Grassmann, and Clifford for computer vision and graphics. CRC Press.

Lavor, C., 2020. Comments on: distance geometry and data science. TOP 28, 340–345.

Lavor, C., Alves, R., 2019. Oriented conformal geometric algebra and the molecular distance geometry problem. Advances in Applied Clifford Algebra 29, 1–19.

Lavor, C., Alves, R., Souza, M.F., Aragon, J.L., 2020. NMR protein structure calculation and sphere intersections. Computational and Mathematical Biophysics 8, 89–101.

Lavor, C., Liberti, L., Donald, B., Worley, B., Bardiaux, B., Malliavin, T., Nilges, M., 2019. Minimal NMR distance information for rigidity of protein graphs. Discrete Applied Mathematics 256, 91–104.

Lavor, C., Liberti, L., Maculan, N., Mucherino, A., 2012a. The discretizable molecular distance geometry problem. Computational Optimization and Applications 52, 115–146.

Lavor, C., Liberti, L., Maculan, N., Mucherino, A., 2012b. Recent advances on the discretizable molecular distance geometry problem. European Journal of Operational Research 219, 698–706.

Lavor, C., Liberti, L., Mucherino, A., 2013. The interval BP algorithm for the discretizable molecular distance geometry problem with interval data. Journal of Global Optimization 56, 855–871.

Lavor, C., Souza, M., Aragon, J.L., 2021a. Orthogonality of isometries in the conformal model of the 3d space. Graphical Models 114, 101100–101106.

Lavor, C., Souza, M., Carvalho, L.M., Gonçalves, D.S., Mucherino, A., 2021b. Improving the sampling process in the interval branch-and-prune algorithm for the discretizable molecular distance geometry problem. Applied Mathematics and Computation 389, 125586.

Li, H., Hestenes, D., Rockwood, A., 2001. Geometric computing with Clifford algebras. Springer. chapter Generalized homogeneous coordinates for computational geometry. pp. 25–58.

Liberti, L., 2020. Distance geometry and data science. TOP 28, 271–339.

Liberti, L., Lavor, C., Maculan, N., 2008. A branch-and-prune algorithm for the molecular distance geometry problem. International Transactions in Operational Research 15, 1–17.

Liberti, L., Lavor, C., Maculan, N., Mucherino, A., 2014. Euclidean distance geometry and applications. SIAM Review 56, 3–69.

Mackay, A., 1974. Generalized structural geometry. Acta Crystallographica Section A 30, 440–447.

Maioli, D., Lavor, C., Gonçalves, D., 2017. A note on computing the intersection of spheres in $\mathbb{R}^n$. ANZIAM Journal 59, 271–279.

Malliavin, T., Mucherino, A., Lavor, C., Liberti, L., 2019. Systematic exploration of protein conformational space using a distance geometry approach. Journal of Chemical Information and Modeling 59, 4486–4503.

Mucherino, A., Lavor, C., Liberti, L., Maculan, N., 2013. Distance geometry: theory, methods, and applications. Springer.

Nielsen, J., Roth, B., 1999. On the kinematics analysis of robotic mechanisms. The International Journal of Robotics Research 18, 1147–1160.

Perwass, C., 2009. Geometric algebra with applications in engineering. Springer.

Sousa, E.V., Fernandes, L.A.F., 2020. TbGAL: a tensor-based library for geometric algebra. Advances in Applied Clifford Algebras 30, 27.

Strang, G., Borre, K., 2012. Algorithms for global positioning. Wellesley-Cambridge Press.

Worley, B., Delhommel, F., Cordier, F., Malliavin, T., Bardiaux, B., Wolff, N., Nilges, M., Lavor, C., Liberti, L., 2018. Tuning interval branch-and-prune for protein structure determination. Journal of Global Optimization 72, 109–127.